Geological Magazine

www.cambridge.org/geo

Tracing lightning-induced mineralogical and physicochemical changes in a fulgurite using X-ray powder diffraction and Rietveld quantitative phase analysis

Chiara Elmi, Bradely R. Couch and Rachel L. Courtney

Department of Geology and Environmental Science, James Madison University, USA

Original Article

Cite this article: Elmi C, Couch BR, and Courtney RL. Tracing lightning-induced mineralogical and physicochemical changes in a fulgurite using X-ray powder diffraction and Rietveld quantitative phase analysis. *Geological Magazine* **163**(e54): 1–9. https://doi.org/10.1017/S0016756826100934

Received: 13 January 2026 UTC
Revised: 7 July 2026 UTC
Accepted: 30 July 2026 UTC

Keywords:
Fulgurite; electrical discharge processes; shock metamorphism; X-ray powder diffraction; Rietveld analysis

Corresponding author:
Chiara Elmi; Email: elmicx@jmu.edu

Abstract

A sample of an elongated, hollow, tube-like fulgurite (labelled NC-CH) was collected in the shorelines' sand of Outer Banks, NC (USA). The goal of this study is to shed light on the origin of this material and phase transformations induced by lightning discharge. X-ray powder diffraction (XRPD) coupled with Rietveld quantitative phase analysis of the surrounding sand (NC-sand) identified quartz, plagioclase, biotite, cordierite and calcite. XRPD analysis of NC-CH revealed stishovite, absent in NC-sand, unequivocally confirmed through high-resolution XRPD and Rietveld quantitative phase analysis. The fulgurite exhibits a high X-ray amorphous abundance (85.3(4) wt%) compared to the sand (49.3(2) wt%), indicating melting and partial melting of primary minerals such as quartz, plagioclase, phyllosilicates and cordierite. Scanning electron microscopy (SEM) with energy dispersive spectrometry (EDS) revealed well-crystallized pyrite clusters (<1 μm) in NC-CH. Pyrite precipitation likely resulted from reducing conditions during sulfidation of ferromagnesian silicates in the presence of H_2S fluids derived from hydrocarbons, water vapour and organosulfur compounds from burned organic matter. By investigating shock-impacted minerals at the nanometric scale, this study provides new insights into physicochemical constraints influencing mineral formation and phase transitions during extreme events such as lightning strikes or meteor impacts.

1. Introduction

The experiments performed by researchers worldwide during the last 60 years have greatly advanced knowledge concerning the formation and behaviour of lightning flashes. However, many pieces of the puzzle pertinent to the mechanism of lightning flashes are still missing, and many of the theories trying to explain its characteristics are mainly of qualitative nature (Cooray, 2014).

The global flash rate of 100 flashes per second over the entire Earth's surface underscores the prevalence of lightning and its potential impact on various environments, including the formation of fulgurites when lightning strikes the ground (Uman and Rakov, 2003). Fulgurites are glassy materials that can be used to better understand the cloud-to-ground (CG) lightning features. When CG lightning strikes an appropriate target material such as sand, soil or rock, the current flows through the target, heating the material to temperatures that exceed its melting point, followed by rapid cooling that results in quenching to form a glass called fulgurite (or petrified lightning). Pasek and Pasek (2018) expanded the definition of fulgurites to include those that are formed by any high-power electric discharge and target materials not typically found in nature. The existence of fulgurites provides direct evidence that materials can be altered thermally and mechanically by a high-current arc discharge.

The mineralogical assemblage and chemical composition of the source materials play a crucial role in the formation of different types of fulgurite. Pasek *et al.* (2012) classified five types of fulgurites based on their morphological features to better understand the properties of lightning strikes that form fulgurites. These authors identified sand fulgurites (type I) with thin, glass walls, clay fulgurites (type II) which consist of thick melted rich walls, caliche fulgurites (type III) that display thick glass poor walls, rock fulgurites (type IV), that are a glassy layer surrounding partially melted rock, and droplet fulgurites (type V) that are morphologically dissimilar from the other four types, but compositionally similar to the type II or IV fulgurites.

Fulgurites provide valuable insights into the power of CG lightning and the processes involved in high-temperature geological transformations. Studying different types of fulgurites can shed light on the extreme conditions that lead to the formation of natural glasses. Fulgurites can be used to study the properties of electrical pulses (*e.g.*, lightning strikes) that created them and, in turn, can help to elucidate quantitative information such as heat transfer, mineral reaction kinetics and energy distribution at the boundary of material constituents. Several

© The Author(s), 2026. Published by Cambridge University Press. This is an Open Access article, distributed under the terms of the Creative Commons Attribution-NonCommercial-NoDerivatives licence (https://creativecommons.org/licenses/by-nc-nd/4.0/), which permits non-commercial re-use, distribution, and reproduction in any medium, provided that no alterations are made and the original article is properly cited. The written permission of Cambridge University Press or the rights holder(s) must be obtained prior to any commercial use and/or adaptation of the article.

Downloaded from https://www.cambridge.org/core. UNIVERSIDAD AUTONOMA METROPOLITANA, on 16 Nov 2026 at 21:40:33, subject to the Cambridge Core terms of use, available at https://www.cambridge.org/core/terms. https://doi.org/10.1017/S0016756826100934

authors studied different types of fulgurite showing that the original parent rock is morphologically and chemically altered and high-temperature mineral phases and amorphous material are produced (Jones *et al.* 2005; Martin Crespo *et al.* 2009; Pasek *et al.* 2012; Chen *et al.* 2017; Elmi *et al.* 2017; Elmi *et al.* 2018; Feng *et al.* 2019; Çalişkanoğlu *et al.* 2024; Morana *et al.* 2025).

Systematic characterization of fulgurites can provide significant insights into shock metamorphism effects as well as into the behaviour of lightning strikes (Pasek and Pasek, 2018; Roberts *et al.* 2019). Shocked samples are rare in Earth's rock record, making lightning-induced materials like fulgurites valuable analogues for impact processes. These materials experience sudden increases in pressure and temperature, similar in intensity and duration to those generated by meteor impacts (Roberts *et al.* 2019). The mineral phase transitions and recrystallization as well as the chemical composition of fulgurites, their microstructure and texture can elucidate the physical and mechanical damage implications of a lightning strike on planetary and Earth materials. The intense conditions during a fulgurite formation lead to substantial geochemical changes, including the loss of volatile elements and the retention of refractory elements (Pasek and Hurst, 2016). However, precise identification of crystalline and amorphous phases in the fulgurites complex systems require the use of analytical methods that do not leave space for confusion. This study applies X-ray powder diffraction (XRPD) and Rietveld quantitative phase analysis to a fulgurite from the Outer Banks, NC (USA), to extend the knowledge about the physicochemical conditions under which fulgurites form. This paper provides the first comprehensive mineralogical and physicochemical investigation of the unique microfeatures of a fulgurite formed by CG lightning strikes in the Southern Shores beach sand in the Outer Banks, NC (USA).

2. Materials and methods

2.a. Geologic setting

The Outer Banks of North Carolina (USA) formed through the combined effects of large-scale longshore sediment transport (spit growth) and beach emergence. Located along a passive continental margin, the Outer Banks were formed by global sea level changes and the accumulation of a large volume of sediments, a range of coastal features, including beaches, inlets, washover deposits, estuaries or sounds, dunes and capes. The barrier islands of the Outer Banks, NC, result from complex interconnected forces, such as sediment availability, storm and wind intensity, and variations in sea level. The areas located behind the Outer Banks are water bodies protected from the open ocean by sandy barrier islands. Inlets are formed when storm surges and high waves drive water across the islands to the estuaries. Beach sand is continuously moved offshore, onshore and along the prevailing longshore currents. Hicks and Crosby (1975) observed that periodic cycles of erosion and deposition occur alongside a longer-term trend of rising sea levels. This gradual increase leads to the submergence of beaches, shoreline retreat and the landward movement of barrier islands. The barrier islands of the Outer Banks are made of sedimentary layers primarily composed of medium-size quartz sand, along with a small proportion of heavy minerals (*e.g.*, zircon, ilmenite, rutile, cordierite, sillimanite and garnet), gravel and shell fragments (Dolan and Lin, 2000). Beach material is transported and deposited in layers through storm overwash or the movement of currents that flow through inlets. According to Moslow and Heron (1978), saline water and sediment flow through the inlets from the ocean side of the barrier islands to the sounds. Bedded within the layers of beach material are units of well-sorted fine-sized sands and silts that are transported by the wind. The deposits that accumulate in these inlets make up approximately 20–25% of the sediments found in the barrier islands (Dolan and Lin, 2000).

According to Dillon and Oldale (1978) peat deposits and tree stumps, remnants of forest stand which generally occur on the back side of barrier islands are presently being found on open ocean beaches. Approximately 14 000 to 18 000 years ago, the melting of glaciers led to a rapid rise in sea levels, triggering the Holocene marine transgression. This process gave rise to extensive chains of Holocene barrier islands in areas near Cape Hatteras, Southern Shores, Colington, Nags Head Woods, Avon, Frisco and Ocracoke. As sea levels continue to rise nowadays, most of the Outer Banks are shifting landward due to washover and inlet processes. Thus, remnants of maritime forests that once occupied the back side of the islands are being uncovered on the beach side.

2.b. Sampling location

In 2021, a solid sample that resembles a root and has a central hollow tube was found on the sand beach in the Southern Shores (36° 10′ 34.47″ N, 75° 44′ 52.98″ W) on the Outer Banks, North Carolina (USA) (Figure 1a). The sample was found by Professor S. Edwin Baird in loose sand between the dunes and the shoreline (Figure 1b). The sample analysed is labelled NC-CH. The beach sand was collected in the same area and labelled NC-sand. NC-CH shows a medium grey colour, and it is an elongated, hollow, glass-lined tube, surrounded by a fine-grained matrix of quartz sand (Figure 2). The intense heat of lightning can vaporize the sand that is struck by lightning, creating hollow glassy space inside the fulgurite which represents the path of lightning propagation into the target material.

2.c. X-ray powder diffraction (XRPD)

X-ray powder diffraction (XRPD) combined with Rietveld quantitative phase analysis was selected as the primary analytical technique due to its ability to provide quantitative and unambiguous identification of crystalline phases and X-ray amorphous abundance in complex systems such as fulgurites. Rietveld refinement applies least-squares whole-pattern fitting to quantify the wt.% of crystalline phases and estimate X-ray amorphous abundance (Rietveld, 1969). Amorphous materials in X-ray analysis are typically characterized by the presence of nanometer-scale crystalline materials. As a result, instead of producing sharp and well-defined diffraction peaks like fully crystalline materials, they display broad humps with large full width at half maximum (FWHM).

XRPD identified NC-sand and NC-CH mineralogical composition. X-ray diffractograms were collected at room temperature using a Malvern PANalytical Empyrean diffractometer equipped with an X'Celerator detector and Cu*K*α radiation (45 kV/40 mA) at the Department of Geology and Environmental Science, James Madison University. A Malvern PANAlytical Bragg-Brentano^{HD} incident beam optical module improved the peak-to-background ratio and the intensity. Analyses of the samples were carried out with spinner-mode analysis (spin rotation at 1 second), a 2θ scan range between 3° and 70°, a step size of 0.02° 2θ, a divergence slit of 0.5°, and incident beam anti-scatter slits of 0.25°. The fitted peak width for collected data was about 0.01° 2θ. Mineral identification was performed using Malvern PANalytical's HighScore Plus

Downloaded from https://www.cambridge.org/core. UNIVERSIDAD AUTONOMA METROPOLITANA, on 16 Nov 2026 at 21:40:33, subject to the Cambridge Core terms of use, available at https://www.cambridge.org/core/terms. https://doi.org/10.1017/S0016756826100934

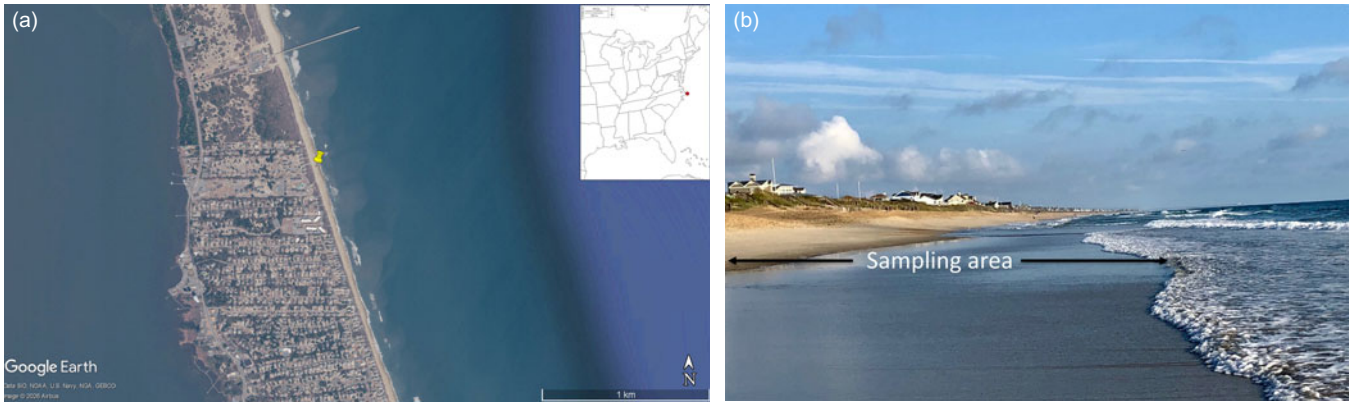


Figure 1. (a) Satellite map showing the sampling location in the Southern Shores, North Carolina (USA) 36° 10′ 34.47″ N 75° 44′ 52.98″ W, elevation 6 m. Map generated with Google Earth Pro 7.3.7.1155 (2026) (McClendon and Jones, 2026). Yellow pin in the map indicates sampling location. Blank map on the upper right adapted from (Dalet, 2026). (b) Close-up view of the sampling site on the beach in Southern Shores, Outer Banks, North Carolina (USA). The arrows show the area where NC-CH and NC-sand were collected. Photo credit: Professor S. Edwin Baird.



Figure 2. Sample NC-CH. Sample is shown in multiple orientations to emphasize its morphological features. Sample's morphology consists of an elongated, hollow tube lined with glass, encased in a fine-grained matrix of quartz sand and some shell fragments.

version 4.9 software (Degen *et al.* 2014) and ICDD PDF-5+ Powder Diffraction File database.

Quantitative phase analyses (Rietveld refinement) and determination of the X-ray amorphous material abundance with the K-factor method after O'Connor and Raven (1988) were performed using Malvern PANalytical HighScore Plus version 4.9 software (Degen *et al.* 2014). Pure crystalline Al_2O_3 was chosen as an external standard and was analysed under the same instrumental conditions as the samples. Rietveld refinement (full-pattern fitting method) uses all observed diffraction data, including peak positions, intensities and shapes, to refine a structural model (Rietveld, 1969). This approach ensures that every reflection in the diffractogram contributes to the fit, eliminating ambiguity and preventing mineral phase misidentification caused by overlapping peaks (Rietveld, 1969; Bish and Howard, 1988; Bish and Post, 1989; Howard and Preston, 1989; Bish and Post, 1993; Young, 1995). Analysis of mixtures yielded high-precision results, with errors generally less than 1.0% absolute (Bish and Howard, 1988; Howard and Preston, 1989). It is worth noting that if an incorrect phase is introduced in the pattern, the refinement fails to converge (Rietveld, 1969; O'Connor and Raven, 1988; Bish and Post, 1989; Howard and Preston, 1989; Bish and Post, 1993; Young, 1995; Toby, 2006). Therefore, the full-pattern fitting method provides a robust basis for phase identification, often making the use of additional techniques redundant for confirming minerals' assemblages.

2.d. Optical microscopy and scanning electron microscopy (SEM)

Polished thin sections (~30 mm thick) of NC-CH were initially investigated with a petrographic microscope in plane-polarized and cross-polarized light.

An uncoated polished slice of NC-CH (0.5 cm thickness) was mounted on carbon tape attached to a stub and examined with a ZEISS Gemini SEM 360VP Scanning Electron Microscope (SEM). This instrument is equipped with a field emission gun and a Gemini 1 electron optical column and is located in the Department of Geology and Environmental Science at James Madison University. Backscattered electron (BSE) images were collected under high vacuum conditions at an accelerating voltage of 15 kV. Data were processed using ZEISS SmartSEM software. An Oxford Instruments Energy Dispersive X-ray spectrometry (EDS) detector was used to determine the chemical composition of the minerals in the samples.

3. Results

A concentric pattern of glassy material was observed both macroscopically (Figure 2) and in thin section analysis via polarizing microscope (Figure 3a) around the hollow, glass-lined tube in NC-CH. The colour of the glass matrix could be ascribed to the melting

Downloaded from https://www.cambridge.org/core. UNIVERSIDAD AUTONOMA METROPOLITANA, on 16 Nov 2026 at 21:40:33, subject to the Cambridge Core terms of use, available at https://www.cambridge.org/core/terms. https://doi.org/10.1017/S0016756826100934

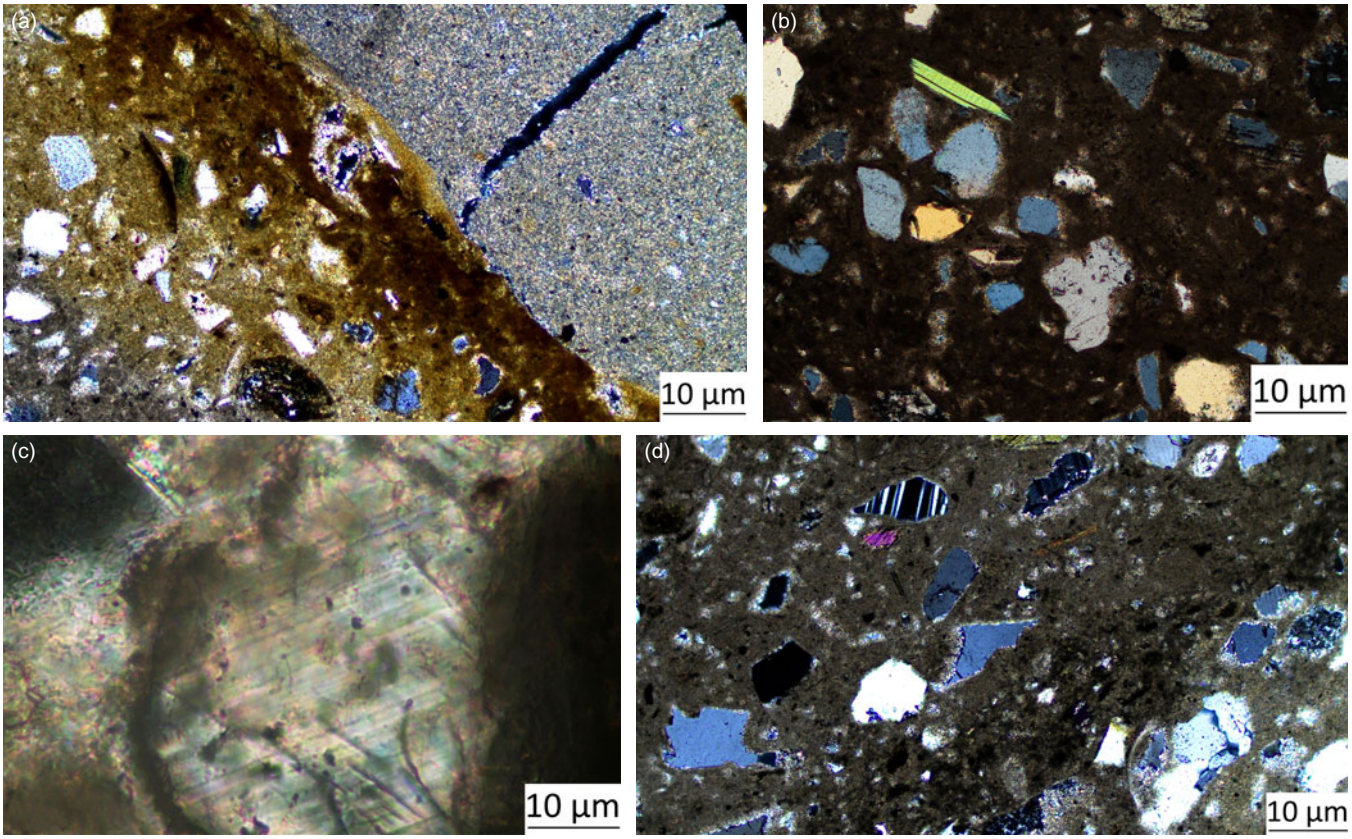


Figure 3. Cross-polarized light image of NC-CH showing: (a) concentric pattern of glassy material around the hollow, glass-lined tube rim. The colour of glass matrix is red owing to the melting of iron-bearing minerals in parent sand; (b) rounded quartz grains as well as residual chloritized biotite observed in the centre of the sample about 2 cm far from the hollow, glass-lined tube; (c) planar deformation features (PDFs) in a quartz crystal located inside glass-lined hollow tube; (d) single residual plagioclase crystal with typical albite twinning observed in the centre of the sample about 2 cm far from the hollow tube rim.

of iron-bearing minerals like biotite in the parent sand during the intense heat of a lightning strike (Figure 3a). Polarizing microscopy in cross-polar light showed that NC-CH displays very fine-grained layers containing tiny, optically unidentifiable crystals as well as quartz and residual chloritized biotite (Figure 3b). Quartz grains in NC-CH are finely fractured and contain fluid inclusions (Figure 3c). The morphology of quartz grains observed in NC-CH (Figure 3b) is rounded, suggesting partial melting and subsequent rapid cooling. Under crossed polarizers, albite lamellar twinning is visible in a single residual plagioclase crystal found about 2 cm far from the hollow tube rim (Figure 3d).

XRPD was chosen for mineralogical analysis because of its inherent ability to analyse fine-grained and complex crystalline mixtures such as fulgurites. High-resolution XRPD analysis was coupled with Rietveld refinement, ensuring accurate identification of minerals and their abundances. This rigorous approach supports the reliability of the data presented in graphical form in Figure 4 and shows the unique features of NC-sand and NC-CH (Figure 5).

The beach sand unaffected by the lightning strike (NC-sand) was analysed using XRPD to determine the mineralogical composition of the parent materials that formed the fulgurite (Figure 5a). The XRPD diffractogram of NC-sand revealed the presence of quartz, plagioclase, cordierite and biotite. NC-sand represents the dominant mineralogical composition of the beach sand at the Outer Banks, NC (USA). The XRPD diffractogram of NC-CH (Figure 5b) showed the presence of quartz and stishovite as well as clinochlore, biotite and calcite. XRPD results on NC-CH confirm thin section observations. XRPD diffractograms of NC-CH showed a d_{001} peak near 14 Å, consistent with clinochlore that was not observed in NC-sand (Figure 5a). The peaks corresponding to $d_{110} = 2.97$ Å, $d_{101} = 2.24$ Å, $d_{110} = 1.97$ Å, that were not observed in NC-sand, are in agreement with published data for stishovite (Holtstam *et al.* 2003). It is important to note that the stishovite identification in NC-CH is unequivocally supported by high-resolution XRPD coupled with Rietveld refinement. Additional techniques such as transmission electron microscopy (TEM), Raman spectroscopy or synchrotron-based diffraction methods were not required to confirm the presence of stishovite in this study, as the Rietveld refinement provided robust phase identification. Although these techniques could offer valuable insights into the amorphous composition, since the Rietveld method only quantifies amorphous abundance, their application falls outside the scope of this work, which focuses on the physicochemical constraints controlling a fulgurite formation in a natural beach environment.

The calcite in NC-CH was ascribed to residual shell fragments embedded in the outside wall of the sample, as also observed with a hand lens (Figure 2). The overall broadening of diffraction peaks observed in NC-CH can be ascribed to a small average crystallite size and general poor crystallinity.

The high X-ray amorphous abundance calculated via Rietveld refinement (Figure 4) in NC-CH (85.3(4) wt%) compared to the unaffected sand (49.3(2) wt%) suggests that the sand underwent sudden Joule heating (*i.e.*, conversion of electrical energy into heat as lightning current passes through low-conductivity sand), which

Downloaded from https://www.cambridge.org/core. UNIVERSIDAD AUTONOMA METROPOLITANA, on 16 Nov 2026 at 21:40:33, subject to the Cambridge Core terms of use, available at https://www.cambridge.org/core/terms. https://doi.org/10.1017/S0016756826100934

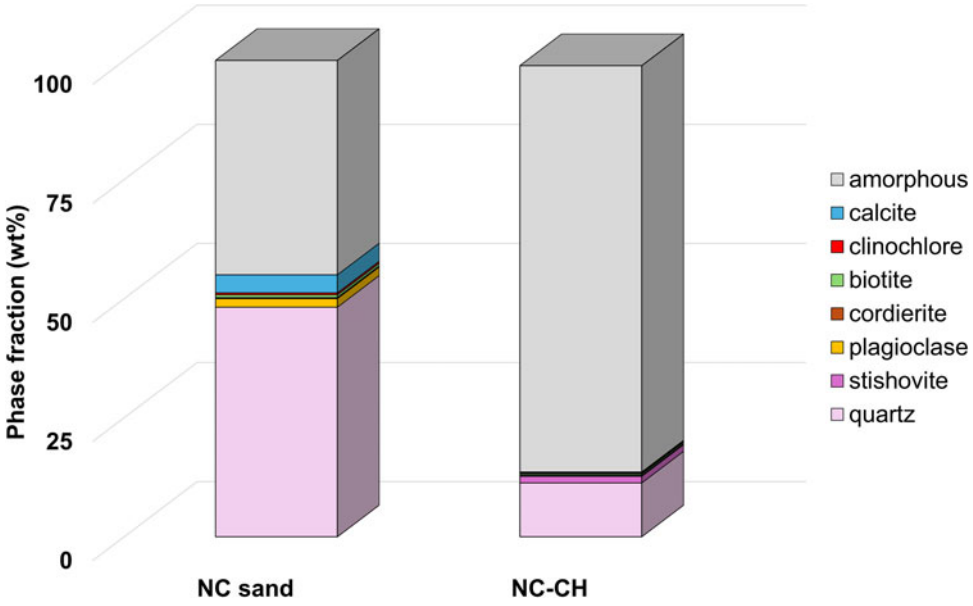


Figure 4. Relative abundances of main mineral phases (>1%) in NC-sand and NC-CH samples calculated via Rietveld analysis.

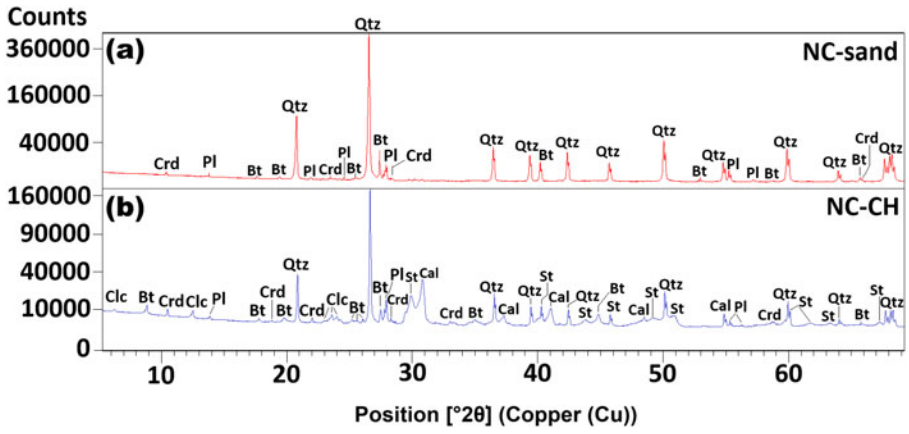


Figure 5. (a) X-ray powder diffraction diffractogram for NC-sand. Mineral abbreviations from Whitney and Evans (2010): Qtz = quartz; Pl = plagioclase; Crd = cordierite; Bt = biotite. (b) X-ray powder diffraction diffractogram for NC-CH. Mineral abbreviations from Whitney and Evans (Whitney and Evans, 2010): Pl = plagioclase; Qtz = quartz; Crd = cordierite; St = stishovite; Clc = clinochlore; Bt = biotite; Cal = calcite.

results in melting and partial melting of parent minerals such as plagioclase, phyllosilicates and quartz. The limited vesicular texture observed via SEM imaging suggests relatively slow cooling occurred in the presence of a hydrous vapour phase. According to Pasek *et al.* (2012) classification, NC-CH can be considered a type II fulgurite.

A coccolith was found in NC-CH embedded in the glass matrix close to the fulgurite external wall, about 3 cm far from the hollow glass-lined tube (Figure 6a). Remnant partially melted fragments of quartz were found via SEM in the glassy matrix of NC-CH (Figure 6b). Plagioclase was not detected via SEM in the glassy matrix of NC-CH. SEM imaging in sample NC-CH revealed nano-sized euhedral crystals of pyrite, each less than 1 μm in size (Figure 6c, d), that was not found in thin section analysis, and it was not shown in the XRPD diffractogram of NC-CH. The average chemical composition of pyrite crystals was measured by EDS, and the empirical formula calculated is $(Fe_{0.881}\ Ti_{0.03}\ Ni_{0.03}\ Co_{0.04}\ Cu_{0.003}\ Zn_{0.002})_{\Sigma 0.986}S_2$.

4. Discussion

The barrier islands and inlets of the Outer Banks, NC, experience a mix of ocean water and freshwater from rivers and streams; therefore, the salinity of water in these regions varies depending on the specific location and water source. In estuarine and inlet areas, salinity can range from 0 to 20 parts per thousand (ppt), occasionally nearing the open ocean's salinity of about 35 ppt (Giese *et al.* 1985). The high salinity increases the conduction of electricity more efficiently (Lewis and Perkin, 1981; Rusydi, 2018) and thus can influence the number of lightning strikes in the area, especially during the summer months. Christian (2003) calculated an average of 44 ± 5 lightning flashes (intracloud and CG combined) occurring around the globe every second. Cecil *et al.* (2014) measured via Optical Transient Detector (OTD) and Lightning Imaging Sensor (LIS) that the mean global flash rate from the merged climatology was 46 flashes/s from May 1995 to March 2000. Dare County, North Carolina, where the sample was collected, recorded over 2000 lightning strikes in 2024, according to the Storm Events Database of National Oceanic and Atmospheric Administration (NOAA) (National Oceanic and Atmospheric Administration, 2025). This averages approximately 5.5 lightning flashes per day, underscoring the frequent lightning activity in the Outer Banks region. The unique geological setting of the Outer Banks, with their shallow highly saline waters and sandy beaches, combined with frequent flash floods, not only favours fulgurite

Downloaded from https://www.cambridge.org/core. UNIVERSIDAD AUTONOMA METROPOLITANA, on 16 Nov 2026 at 21:40:33, subject to the Cambridge Core terms of use, available at https://www.cambridge.org/core/terms. https://doi.org/10.1017/S0016756826100934

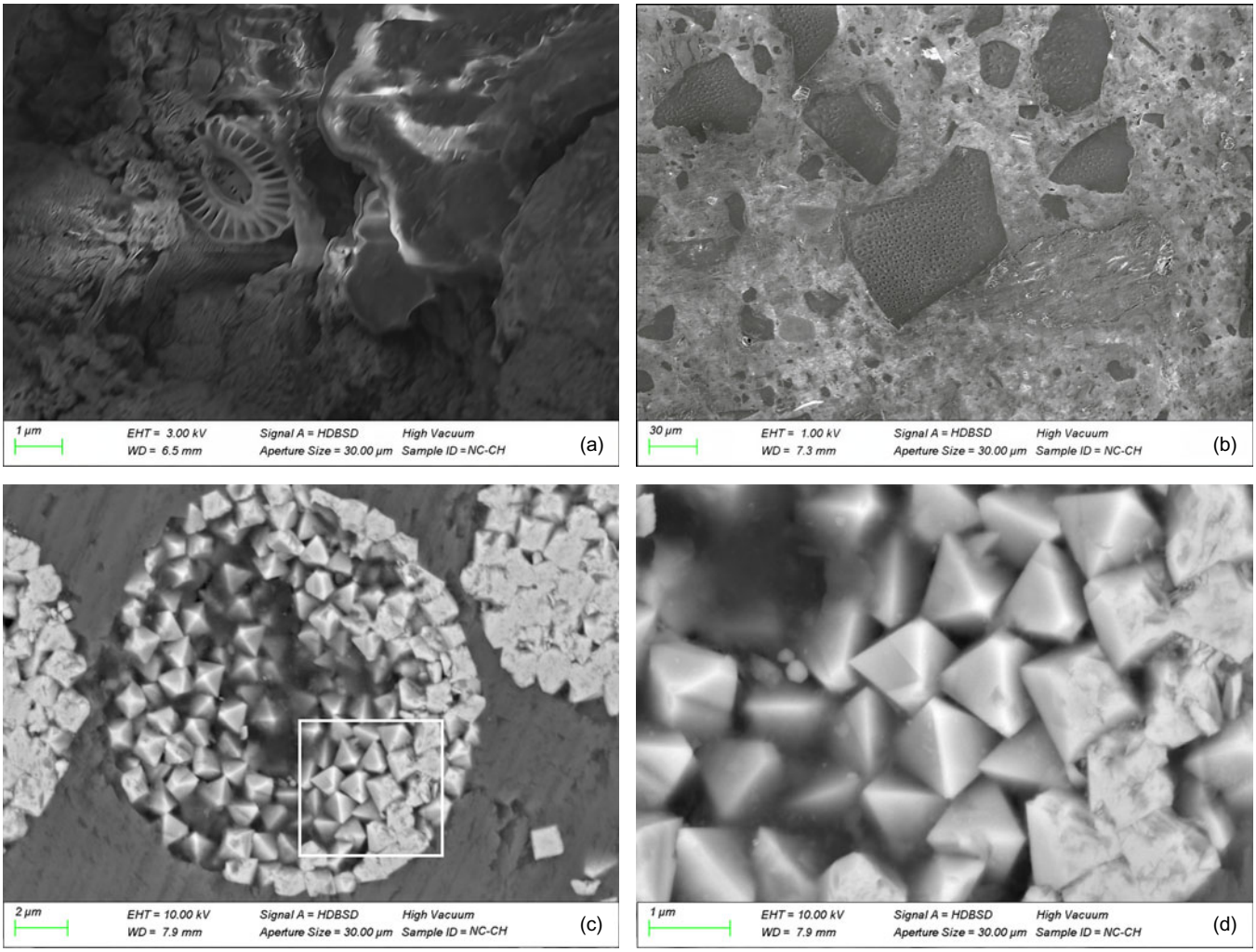


Figure 6. Scanning electron microscopy (SEM) images of NC-CH showing: (a) a coccolith embedded in the glass matrix found close to the fulgurite external wall; (b) fragments of quartz found in the glassy matrix close to the hollow tube rim; (c) framboidal pyrite crystals less than 1 µm in size found embedded in vesicles in the glass matrix about 2 cm far from the hollow tube rim and about 1 cm below the fulgurite external wall; (d) detail of the euhedral pyrite crystals.

formation but also amplifies the effects of lightning-induced shock waves, which record distinct physical and chemical features on affected minerals.

Lightning generates a shock wave through rapid air expansion, propelling compressed air outwards at supersonic speeds (Glass, 1974). As the shock wave expands, pressures decrease rapidly and, when it meets a surface that is in line-of-sight of the point of impact, it is reflected and amplified (Chipley *et al.* 2013). Shock events such as lightning, meteor impacts, and explosions produce extreme pressures and temperatures that drive rapid mineral transformations, including phase transitions and vaporization (Langenhorst, 2002; Stöffler *et al.* 2018). Lightning temperatures often exceed quartz's melting point (1600–2000°C), influenced by moisture content (Chen *et al.* 2017; Elmi *et al.* 2017; Elmi *et al.* 2018). Genareau *et al.* (2020) linked lightning-induced textures in volcanic ash to both thermal effects and shock wave expansion, which can double the discharge channel radius. In sample NC-CH, a lightning-induced shock wave in Outer Banks beach sand produced concentric glass layers radiating from a hollow centre (Figures 2 and 3a). These glass layers formed during the transient high-temperature and high-pressure conditions experienced during a lightning strike.

The interactions of minerals in Earth materials with lightning are essential for understanding the nature of the lightning environment near and at the point of a direct strike. The thermal impact depends on the material's chemistry, temperature and pressure rise, moisture and salinity levels, and time needed to melt the beach sand. Mineral assemblages revealed via XRPD and Rietveld refinement in NC-CH (Figure 5b) are essential for reconstructing the physicochemical pathways under which the fulgurite formed in the beach sands of the Southern Shore in the Outer Banks, NC. The XRPD diffractogram of NC-sand (Figure 5a) reveals the dominant mineralogical composition of beach sand from the Outer Banks, NC (USA). Accurate identification of crystalline phases in the unshocked reference samples was essential for recognizing residual shocked minerals in NC-CH. Rietveld refinement was conducted on NC-sand and NC-CH by fitting a calculated diffractogram to the observed data by adjusting each of the variables to minimize the difference between the calculated and observed XRPD diffractograms. The calculated high X-ray amorphous abundance in NC-CH compared to the lower amount in the unaffected sand (Figure 4) indicates that NC-sand was subjected to the melting and partial melting of primary minerals such as quartz, plagioclase, phyllosilicates and cordierite.

Downloaded from https://www.cambridge.org/core. UNIVERSIDAD AUTONOMA METROPOLITANA, on 16 Nov 2026 at 21:40:33, subject to the Cambridge Core terms of use, available at https://www.cambridge.org/core/terms. https://doi.org/10.1017/S0016756826100934

Comparison of the two diffractograms (Figure 5) and the Rietveld refinement results (Figure 4) show a significant difference in X-ray amorphous materials and the plausible presence of stishovite in NC-CH, representing the first reported identification of this mineral in a fulgurite.

Coesite and stishovite are key indicators of ultrahigh-pressure metamorphism, with stishovite being more stable than coesite above ~8–9 GPa and at temperatures ≥1200°C (Mosenfelder and Bohlen, 1997; Stevens *et al.* 1997; Chen *et al.* 2010; Ono *et al.* 2017; Folco *et al.* 2018). The combination of stishovite formation, reduced amount of quartz and increased X-ray amorphous abundance observed in NC-CH (Figure 4) suggests that NC-sand underwent a high-energy, rapid shock from an arc discharge wave. Stishovite is a metastable high-pressure polymorph of SiO_2 at ambient conditions; therefore, its presence (1.6(3) wt%) in NC-CH is an indicator of a peak shock pressure that created the fulgurite when lightning struck the beach sand.

XRPD data (Figure 5) coupled with Rietveld refinement results (Figure 4) of NC-CH indicates distinct physical and chemical conditions of shock-wave environments captured in the SiO_2 polymorph stishovite. Fulgurites are rare and inherently heterogeneous materials. Therefore, the rapid and highly localized heating associated with their formation can result in significant variability in mineral assemblages and textures, even between samples at the same location. The occurrence of stishovite in NC-CH, particularly in areas where the shock-wave rim is well preserved, provides important insights into localized pressure–temperature conditions and the transient processes governing mineral formation under extreme, non-equilibrium conditions. High-temperature SiO_2 polymorphs are stable between 1470°C and 1705°C, following the sequence: α-quartz → β-quartz (573°C) → β-tridymite (870 °C) → β-cristobalite (1470°C) (Pagliari *et al.* 2013). At room temperature, α-cristobalite remains stable up to ~1.6 GPa, transitioning to β-cristobalite above this pressure. (Downs and Palmer, 1994). Temperatures above ~1000°C are needed to constrain the coesite–stishovite equilibrium boundary (Zhang *et al.* 1996). Experiments at 10 GPa and 1000°C on silica glass–water mixtures produced stishovite containing ~1.3 wt% structural water (Spektor *et al.* 2011). While these conditions apply to pure SiO_2 polymorphs, plagioclase in NC-sand (Figure 5a) acts as a flux, lowering quartz's melting point to 1100–1200°C, especially in the presence of water (Darling *et al.* 1997; Dapiaggi *et al.* 2015; Yan and Zhou, 2015).

The formation and metastability of stishovite under shock conditions were documented in impact structures, where the interplay of conductive heating and shock reverberation contribute to its preservation (Stähle *et al.* 2008). Litvin *et al.* (2024) showed that stishovite can remain metastable under terrestrial conditions, particularly when formed during high-pressure events such as arc discharges or impacts. Shock compression experiments using *in situ* X-ray diffraction showed that crystalline stishovite can retransform during shock pressure release to quartz or become amorphous to a dense glass at elevated temperatures (Tracy *et al.* 2018). Its ultrafast formation (<1 μs) was observed in short-duration shocks (Mansfeld *et al.* 2017). These conditions suggest that stishovite can both rapidly crystallize and be stable under transient high-pressure conditions. The broad and low-intensity peaks of stishovite observed in NC-CH (Figure 5b) suggest that the arc discharge created conditions suitable for stishovite formation and the rapid shock release preserved before complete reversion to quartz or an amorphous phase could occur.

XRPD diffractogram of NC-sand (Figure 5a) showed the presence of cordierite which was also found as a residual phase in NC-CH (Figure 5b). Cordierite forms under stress conditions similar to those in lower granulite facies metamorphism (Wynne-Edwards and Hayi, 1962; Hess, 1969; Young *et al.* 1989), where it can coexist with quartz. Seifert and Schreyer (1970) identified the assemblage Al silicate + chlorite + quartz as optimal for cordierite formation at <0.5 GPa water pressure and temperatures between 450°C and 1300°C. The coexistence of residual cordierite with quartz and stishovite in NC-CH suggests a unique high-pressure, high-temperature environment consistent with shock-impact conditions. The mineral assemblage observed via XRPD and Rietveld refinement in NC-CH suggests that the formation of NC-CH occurred at temperatures ranging from 900°C to 1200°C and pressures near or above 6 GPa.

SEM imaging of NC-CH revealed nano-sized euhedral pyrite crystals within spherical voids in the glass matrix (Figure 6c,d), undetected by XRPD. Their formation could occur under reducing conditions during a lightning strike, driven by sulfidation of ferromagnesian silicates (e.g., clinochlore, cordierite, biotite) in the presence of H_2S from anoxic organic matter decomposition (Sassano and Schrijver, 1989). High temperatures (800–1200°C) and water vapour can generate H_2S, while CO acts as a reducing agent (Yu *et al.* 2015), enhancing sulfurization reactions (Renggli *et al.* 2018; Huang *et al.* 2020). During the combustion of organic matter, aromatic carbon compounds and organosulfur complexes can form, including SO_2, H_2S and sulphur-bearing organics (Hussain *et al.* 2024). Framboidal pyrite may result from hydrocarbon droplets in aqueous solutions trapped within vesicles in the glass matrix. Data suggest that the formation of pyrite nanocrystals in NC-CH (Figure 6c,d) was facilitated by the incorporation of CO into sulfurization reactions involving ferromagnesian silicates (*e.g.*, clinochlore, cordierite, biotite) in the presence of organic matter.

5. Conclusions

Shock-wave effects have been observed in common rock-forming and some accessory minerals in rocks subjected to explosive hypervelocity impacts. Lightning causes a rapid expansion of air, generating a shock wave. The outcomes of this study provided new insights into quantitative aspects of high current discharge processes on rocks and mineral phase transitions. The fulgurites from the Outer Banks, NC (USA), exhibit textural, mineralogical and chemical characteristics that are significantly different from those of typical sand fulgurites formed by lightning strikes. Unlike the predominantly glassy, tubular structures commonly observed, these specimens display heterogeneous textures with crystalline phases scattered within a fine-grained material. These distinctive features have led to ongoing debate regarding the origin of the fulgurite from the Outer Banks, NC (USA), questioning whether they represent fulgurites or products of biological activity. In this paper, XRPD combined with Rietveld refinement showed the presence of stishovite, a mineral typically associated with impact structures and extreme pressure conditions, alongside unexpected secondary phases such as framboidal pyrite which crystal are less than 1 μm in size within spherical void inside the fulgurite glassy matrix. The application of XRPD combined with Rietveld refinement provides a robust, quantitative approach for eliminating ambiguity in phase identification and establishing the combination of these two methods as a reliable standard for characterizing complex mineral assemblages.

The mineralogical features of NC-CH from the Southern Shores in Outer Banks, NC (USA), provide insights into the physical–chemical effects occurring in rocks and sediments in

Downloaded from https://www.cambridge.org/core. UNIVERSIDAD AUTONOMA METROPOLITANA, on 16 Nov 2026 at 21:40:33, subject to the Cambridge Core terms of use, available at https://www.cambridge.org/core/terms. https://doi.org/10.1017/S0016756826100934

response to shock-impact events such as a lightning strike. The sample studied displays the effects of shock wave-related processes owing to lightning impact on the shoreline beach fine-grained sand, supporting the genesis of NC-CH. XRPD analyses of the NC-CH sample revealed mineral assemblages that clarified the reactivity and temperature range at which the fulgurite formed in the beach sands. The association of quartz and high-pressure polymorph stishovite as revealed by Rietveld refinement is reliable mineralogical evidence for a shock-impact origin of NC-CH. Data suggest that NC-CH formed at temperatures between 900°C and 1200°C and pressures near or above 6 GPa. These conditions suggest the transit of a shock wave that results in a shutter cone that radiates from the point of impact with a sudden increase in pressure and temperature followed by a rapid decrease.

The sulfurization reaction at temperatures exceeding 800°C in the presence of ferro-magnesian minerals, combined with the incorporation of hydrocarbons and CO from the burning of organic matter trapped in bubbles, led to the precipitation of framboidal pyrite. When lightning strikes the beach sand at the Outer Banks, NC (USA), the combustion of organic matter could lead to the formation of aromatic carbon compounds and organosulfur complexes. Sulphur present in organic matter can combine carbon and hydrogen with the water vapour to create various organosulfur compounds. Data indicate that interactions among hydrocarbons, water vapour and organic matter trapped within the vesicles of NC-CH may promote the formation of organosulfur compounds. These compounds can subsequently react with melting clinochlore, biotite and cordierite, leading to the formation of framboidal pyrite.

Acknowledgements. The authors thank Professor S. Edwin Baird for the sample collection and continuing interest in fulgurites. An anonymous reviewer is kindly acknowledged for the thoughtful comments that greatly improved the quality of the manuscript.

Financial support. This research was supported by the JMU William Frangos Memorial Endowment and JMU Doherty Geology Student Research Endowment.

Competing interests. The authors declare no conflict of interest.

References

Bish DL and Howard SA (1988) Quantitative phase analysis using the Rietveld method. *Journal of Applied Crystallography* **21**(2), 86–91.

Bish DL and Post JE (1989) *Modern Powder Diffraction*, i–xii + 369p. Mineralogical Society of America.

Bish DL and Post JE (1993) Quantitative mineralogical analysis using the Rietveld full-pattern fitting method. *American Mineralogist* **78**(9–10), 932–40.

Çalişkanoğlu AZ, Cimarelli C, Dingwell DB and Camara ASB (2024) Experimental vs. natural fulgurite: A comparison and implications for the formation process. *American Mineralogist* **109**(10), 1682–90.

Cecil DJ, Buechler DE and Blakeslee RJ (2014) Gridded lightning climatology from TRMM-LIS and OTD: Dataset description. *Atmospheric Research* **135–136**, 404–14.

Chen J, Elmi C, Goldsby D and Gieré R (2017) Generation of shock lamellae and melting in rocks by lightning-induced shock waves and electrical heating: Lightning shock and fulgurite formation. *Geophysical Research Letters* **44**(17), 8757–68.

Chen M, Xiao W and Xie X (2010) Coesite and quartz characteristic of crystallization from shock-produced silica melt in the Xiuyan crater. *Earth and Planetary Science Letters* **297**(1–2), 306–14.

Chipley M, Lyon W, Smilowitz R and Williams P (2013) Chapter 4. Explosive blast theory. In *Reference Manual to Mitigate Potential Terrorist Attacks against Buildings* (ed M Chipley), pp. 1–14. Risk Management Series FEMA-428/BIPS-07, Washington, D.C., USA.

Christian HJ (2003) Global frequency and distribution of lightning as observed from space by the optical transient detector. *Journal of Geophysical Research* **108**(D1), 4005.

Cooray V (2014) Mechanism of electrical discharges. In *The Lightning Flash, 2nd ed.*, pp. 41–117. London: Energy Engineering, IET Digital Library.

Dalet D (2026) East coast of the United States. *d-maps. Free maps*. https://www.d-maps.com/carte.php?num_car=5223&lang=en. Accessed 16 June 2026.

Dapiaggi M, Pagliari L, Pavese A, Sciascia L, Merli M and Francescon F (2015) The formation of silica high temperature polymorphs from quartz: Influence of grain size and mineralising agents. *Journal of the European Ceramic Society* **35**(16), 4547–55.

Darling RS, Chou I-M and Bodnar RJ (1997) An occurrence of metastable cristobalite in high-pressure garnet granulite. *Science* **276**(5309), 91–93.

Degen T, Sadki M, Bron E, König U and Nénert G (2014) The HighScore suite. *Powder Diffraction* **29**(S2), S13–S18.

Dillon WP and Oldale RN (1978) Late quaternary sea-level curve: Reinterpretation based on glaciotectonic influence. *Geology* **6**(1), 56–60.

Dolan R and Lin H (2000) *The Outer Banks of North Carolina*, 58p. Reston, Virginia: U.S. Geological Survey.

Downs RT and Palmer DC (1994) The pressure behavior of α-cristobalite. *American Mineralogist* **79**(1–2), 9–14.

Elmi C, Chen J, Goldsby D and Gieré R (2017) Mineralogical and compositional features of rock fulgurites: A record of lightning effects on granite. *American Mineralogist* **102**(7), 1470–81.

Elmi C, Coleman N, Miu K and Schruba E (2018) Experimental simulation of lightning current discharge on rocks. *Applied Sciences* **8**(12), 2394.

Feng T, Lang C and Pasek MA (2019) The origin of blue coloration in a fulgurite from Marquette, Michigan. *Lithos* **342–343**, 288–94.

Folco L, Mugnaioli E, Gemelli M, Masotta M and Campanale F (2018) Direct quartz-coesite transformation in shocked porous sandstone from Kamil Crater (Egypt). *Geology* **46**(9), 739–42.

Genareau K, Gharghabi P and Klüss J (2020) Influence of shock propagation on lightning evidence in volcanic ashfall deposits. *Earth and Planetary Science Letters* **535**, 116124.

Giese GL, Wilder HB and Parker GG Jr (1985) *Hydrology of Major Estuaries and Sounds of North Carolina*. Reston, Virginia: U.S. Geological Survey, 175p.

Glass II (1974) *Shock Waves & Man 1st ed.*, 169p. Toronto: University of Toronto Institute for Aerospace Studies.

Hess PC (1969) The metamorphic paragenesis of cordierite in pelitic rocks. *Contributions to Mineralogy and Petrology* **24**(3), 191–207.

Hicks SD and Crosby JE (1975) An average, long-period, sea-level series for the United States (ed. National Ocean Survey).

Holtstam D, Broman C, Söderhielm J and Zetterqvist A (2003) First discovery of stishovite in an iron meteorite. *Meteoritics & Planetary Science* **38**(11), 1579–83.

Howard SA and Preston KD (1989) Profile fitting of powder diffraction patterns. In *Modern Powder Diffraction* (eds DL Bish and JE Post), pp. 217–75. Reviews in Mineralogy and Geochemistry, Washington, D.C. USA.

Huang L-L, Miao B-K, Chen G-Z, Shao H-M and Ouyang Z-Y (2020) The sulfurization recorded in tridymite in the monomict eucrite Northwest Africa 11591. *Meteoritics & Planetary Science* **55**(7), 1441–57.

Hussain B, Li W, Fang Q and Li Y (2024) Synergistic effects of fuel components on aromatics formation in combustion: A review. *Applied Sciences* **14**(15), 6720.

Jones BE, Jones KS, Rambo KJ, Rakov VA, Jerald J and Uman MA (2005) Oxide reduction during triggered-lightning fulgurite formation. *Journal of Atmospheric and Solar-Terrestrial Physics* **67**(4), 423–28.

Langenhorst F (2002) Shock metamorphism of some minerals: Basic introduction and microstructural observations. *Bulletin of the Czech Geological Survey* **77**(4), 265–82.

Lewis EL and Perkin RG (1981) The practical salinity scale 1978: Conversion of existing data. *Deep Sea Research Part A. Oceanographic Research Papers* **28**(4), 307–28.

Downloaded from https://www.cambridge.org/core. UNIVERSIDAD AUTONOMA METROPOLITANA, on 16 Nov 2026 at 21:40:33, subject to the Cambridge Core terms of use, available at https://www.cambridge.org/core/terms. https://doi.org/10.1017/S0016756826100934

Litvin Yu.A, Spivak AV and Kuzyura AV (2024) Variability of stishovite genesis under terrestrial conditions: physicogeochemical aspects. *Geochemistry International* **62**(2), 124–39.

Mansfeld U, Langenhorst F, Ebert M, Kowitz A and Schmitt RT (2017) Microscopic evidence of stishovite generated in low-pressure shock experiments on porous sandstone: Constraints on its genesis. *Meteoritics & Planetary Science* **52**(7), 1449–64.

Martin Crespo T, Lozano Fernandez RP and Gonzalez Laguna R (2009) The fulgurite of Torre de Moncorvo (Portugal): Description and analysis of the glass. *European Journal of Mineralogy* **21**(4), 783–94.

McClendon B and Jones M (2026) Google Earth Pro for desktop. https://www.google.com/earth/about/versions/#earth-pro. Accessed 16 June 2026.

Morana M, Pasek MA, Catelani T and Bindi L (2025) Mineralogical characterization of the Seffner fulgurite, Florida: Insights into lightning-induced petrogenesis. *American Mineralogist* **110**(7), 1149–57.

Mosenfelder JL and Bohlen SR (1997) Kinetics of the coesite to quartz transformation. *Earth and Planetary Science Letters* **153**(1), 133–47.

Moslow TF and Heron S.D. Jr. (1978) Relict inlets: Preservation and occurrence in the Holocene stratigraphy of Southern core banks, North Carolina. *Journal of Sedimentary Petrology* **48**, 1275–86.

National Oceanic and Atmospheric Administration (2025) Storm Events Database | National Centers for Environmental Information. *Storm events database*. https://www.ncdc.noaa.gov/stormevents. Accessed 14 December 2025.

O'Connor BH and Raven MD (1988) Application of the Rietveld refinement procedure in assaying powdered mixtures. *Powder Diffraction* **3**(1), 2–6.

Ono S, Kikegawa T, Higo Y and Tange Y (2017) Precise determination of the phase boundary between coesite and stishovite in SiO_2. *Physics of the Earth and Planetary Interiors* **264**, 1–6.

Pagliari L, Dapiaggi M, Pavese A and Francescon F (2013) A kinetic study of the quartz–cristobalite phase transition. *Journal of the European Ceramic Society* **33**(15), 3403–10.

Pasek MA, Block K and Pasek V (2012) Fulgurite morphology: A classification scheme and clues to formation. *Contributions to Mineralogy and Petrology* **164**(3), 477–92.

Pasek MA and Hurst M (2016) A fossilized energy distribution of lightning. *Scientific Reports* **6**, 30586.

Pasek MA and Pasek VD (2018) The forensics of fulgurite formation. *Mineralogy and Petrology* **112**(2), 185–98.

Renggli CJ, King PL, Henley RW, Guagliardo P, McMorrow L, Middleton JP and Turner M (2018) An experimental study of SO_2 reactions with silicate glasses and supercooled melts in the system anorthite–diopside–albite at high temperature. *Contributions to Mineralogy and Petrology* **174**(1), 3.

Rietveld HM (1969) A profile refinement method for nuclear and magnetic structures. *Journal of Applied Crystallography* **2**(2), 65–71.

Roberts SE, Sheffer AA, McCanta MC, Dyar MD and Sklute EC (2019) Oxidation state of iron in fulgurites and Trinitite: Implications for redox changes during abrupt high-temperature and pressure events. *Geochimica et Cosmochimica Acta* **266**, 332–50.

Rusydi AF (2018) Correlation between conductivity and total dissolved solid in various type of water: A review. *IOP Conference Series: Earth and Environmental Science* **118**, 012019.

Sassano GP and Schrijver K (1989) Framboidal Pyrite: Early-diagenetic late-diagenetic and hydrothermal occurrences from the Acton Vale quarry, Cambro-Ordovician, Quebec. *American Journal of Science* **289**, 167–79.

Seifert F and Schreyer W (1970) Lower temperature stability limit of Mg cordierite in the range 1–7 kb water pressure: A redetermination. *Contributions to Mineralogy and Petrology* **27**(3), 225–38.

Spektor K, Nylen J, Stoyanov E, Navrotsky A, Hervig RL, Leinenweber K, Holland GP and Häussermann U (2011) Ultrahydrous stishovite from high-pressure hydrothermal treatment of SiO_2. *Proceedings of the National Academy of Sciences* **108**(52), 20918–22.

Stähle V, Altherr R, Koch M and Nasdala L (2008) Shock-induced growth and metastability of stishovite and coesite in lithic clasts from suevite of the Ries impact crater (Germany). *Contributions to Mineralogy and Petrology* **155**(4), 457–72.

Stevens SJ, Hand RJ and Sharp JH (1997) Polymorphism of silica. *Journal of Materials Science* **32**(11), 2929–35.

Stöffler D, Hamann C and Metzler K (2018) Shock metamorphism of planetary silicate rocks and sediments: Proposal for an updated classification system. *Meteoritics & Planetary Science* **53**(1), 5–49.

Toby BH (2006) R factors in Rietveld analysis: How good is good enough? *Powder Diffraction* **21**(1), 67–70.

Tracy SJ, Turneaure SJ and Duffy TS (2018) In situ X-Ray diffraction of shock-compressed fused silica. *Physical Review Letters* **120**(13), 135702.

Uman MA and Rakov VA (2003) Incidence of lightning. In *Lightning: Physics and Effects* (eds MA Uman and VA Rakov), pp. 24–66. Cambridge, Cambridge University Press.

Whitney DL and Evans BW (2010) Abbreviations for names of rock-forming minerals. *American Mineralogist* **95**(1), 185–87.

Wynne-Edwards HR and Hayi PW (1962) Coexisting cordierite and garner in regionally metamorphosed rocks from the Westport area, Ontario. *The Canadian Mineralogist* **7**, 453–78.

Yan Y and Zhou Y (2015) Preparation of cristobalite and its thermal characteristics. In *Proceedings of the 11th International Congress for Applied Mineralogy (ICAM)* (ed. F Dong), pp. 441–45. Cham: Springer International Publishing.

Young ED, Anderson JL, Clarke HS and Thomas WM (1989) Petrology of biotite-cordierite-garnet gneiss of the McCullough range, Nevada I. Evidence for Proterozoic low-pressure fluid-absent granulite grade metamorphism in the Southern Cordillera. *Journal of Petrology* **30**(1), 39–60.

Young RA (ed.) (1995) *The Rietveld Method*. Oxford, New York: Oxford University Press, 308p.

Yu Y, Aykol M and Wolverton C (2015) Reaction thermochemistry of metal sulfides with GGA and GGA+*U* calculations. *Physical Review B* **92**(19), 195118.

Zhang J, Li B, Utsumi W and Liebermann RC (1996) In situ X-ray observations of the coesite-stishovite transition: reversed phase boundary and kinetics. *Physics and Chemistry of Minerals* **23**(1), 1–10.

Downloaded from https://www.cambridge.org/core. UNIVERSIDAD AUTONOMA METROPOLITANA, on 16 Nov 2026 at 21:40:33, subject to the Cambridge Core terms of use, available at https://www.cambridge.org/core/terms. https://doi.org/10.1017/S0016756826100934